

# 1 Sea ice and argon

2  
3 **Clive Hambler**

4 Department of Biology, University of Oxford, UK. ORCID 0000-0002-2361-828X  
5 clive.hambler@biology.ox.ac.uk

## 6 7 **Abstract**

8 1) Atmospheric argon on Earth and Mars cycles on a seasonal basis and abiotic factors will be particularly important  
9 drivers of this noble gas. 2) It is predicted and confirmed that there is similarity in the seasonality of sea ice and  
10 argon, with atmospheric argon in a Hemisphere often increasing fastest when sea ice in that Hemisphere is declining  
11 fastest. 3) There is some visual similarity between the detailed phenology of Greenland Sea ice extent and argon in  
12 some Northern Hemisphere sites, but formal analysis is required. 4) If causal, the mechanism is unclear but could  
13 involve argon bubble formation during freezing and bubble release in the spring melt. 5) Other variables with very  
14 similar phenology to sea ice, including high-latitude sea temperatures, should be investigated as potential drivers. 6)  
15 Cycling of argon by sea ice would strengthen the argument that seasonal cycling of carbon dioxide is in part driven  
16 abiotically.

17  
18 **Keywords** Carbon dioxide • Cycles • Degassing • Outgassing • Polar • Seasonal

## 19 20 **Introduction**

21 Argon, carbon dioxide, oxygen and methane have seasonal cycles on Earth and Mars (Battle et al 2003; Cassar et al  
22 2008; Keeling & Manning 2014; Trainer et al 2019; Hambler & Henderson 2022; Hambler 2022). Cycles of  
23 argon on Earth have been ascribed to outgassing from the warmer ocean water in the summers (Battle et al 2003;  
24 Cassar et al 2008; Stanley et al 2009); argon solubility depends on temperature and salinity (Hamme & Emerson  
25 2004). On Mars, freeze-distillation concentrates atmospheric argon as carbon dioxide condenses in the winter  
26 (Trainer et al 2019). If seasonal cycles of some gases can be driven by freezing cycles on Mars, might the same be  
27 true on Earth?

28  
29 There is at least one mechanism by which sea ice seasonality might influence global atmospheric argon dynamics but  
30 such an effect has not been quantified on a large scale. Degassing as sea water freezes drives argon from water into  
31 brine channels and inclusions in the ice, and bubble nucleation can occur (Zhou et al 2013). Bubbles may diffuse  
32 upwards but some reach impermeable layers of ice, and sea ice can have multiple layers with differing and low  
33 permeability to gases (Moreau et al 2014; Angelopoulos et al 2022). Field observations at Barrow (Alaska) and a  
34 tank experiment suggest bubbles rich in argon can escape sea ice as it melts, leading to the prediction that some  
35 bubbles are released to the atmosphere in an "intense and rapid" spring pulse (Moreau et al 2014).

36  
37 Several other mechanisms influence argon exchange between air, sea and sea ice. Convection patterns in brine (the  
38 'brine convective pump') may amplify argon concentrations within the ice's voids above the concentration in  
39 underlying water and above saturation levels (Vancoppenolle et al 2010; Zhou et al 2013; Tison et al 2016). Snow  
40 melting and subsequent freezing, and flows of air into voids in ice, may also pump argon into sea ice (Zhou et al  
41 2013). Melting ice expels a small amount of argon to the ocean (Moreau et al 2014). After degassing, melting ice  
42 depleted in argon might form a cold-water sink for argon from the atmosphere - but this is very difficult to sample in  
43 the field (Moreau et al 2014). Wind can inject argon in bubbles into sea water (Stanley et al 2009) and wind can  
44 influence gas exchange with sea ice (Vancoppenolle et al 2013).

45

46 I suggest the relatively high amplitude of the annual cycle of atmospheric argon at some high-latitude sites reported  
47 by Battle et al (2003) is consistent with a hypothesized role of sea ice as well as simply with changing ocean  
48 temperature and solubility - although more sampling is required to quantify latitudinal gradients and long-term trends  
49 (Cassar et al 2008).

50

51 If atmospheric argon cycles have a clear phenological (timing) similarity to sea ice within a Hemisphere, the  
52 possibility of an abiotic contribution of sea ice to Earth's carbon cycle would be strengthened: it would suggest sea  
53 ice may have a detectable effect at a planetary scale even on a gas that is an order of magnitude more abundant than  
54 carbon dioxide. Indeed, argon fluxes in sea ice are helpful to elucidating other gas dynamics in ice (Ito et al 2011;  
55 Moreau et al 2014; Tison et al 2016) and the argon cycle can help disentangle seasonal effects of solubility on the  
56 oxygen cycle (Battle et al 2003; Cassar et al 2008).

57

58 On Earth, seasonal cycles of carbon dioxide and oxygen have been widely assumed to be driven by terrestrial  
59 vegetation of the Northern Hemisphere (Keeling 1960; Keeling et al 2001; Buermann et al 2007; Ciais et al 2013;  
60 Keeling & Manning 2014; Keeling & Graven 2021). However, Earth's abiotic seasonal processes involving sea ice  
61 (such as brine rejection, freeze degassing, temperature-dependent solubility and calcium carbonate crystallization)  
62 make a contribution to carbon dioxide fluxes, at least locally (Semiletov et al 2007; Nomura et al 2010; Geilfus et al  
63 2013; Sogaard et al 2013; Vancoppenolle et al 2013; Moreau et al 2016; Brown et al 2015; Tison et al 2016;  
64 Bushinsky et al 2017, 2019; MOSAiC 2019). The effect of sea ice on large-scale carbon dioxide fluxes, if any,  
65 remains unknown but is under investigation (Angelopoulos et al 2022). Due to data limitations and other constraints,  
66 the contribution of sea ice is arguably poorly quantified and incompletely represented in Earth System models  
67 (Vancoppenolle & Tedesco 2016). I have suggested that Earth's global carbon dioxide seasonality may be dominated  
68 by or strongly affected by abiotic processes, given the extremely close similarity of the rates of change of sea ice,  
69 carbon dioxide and methane (Nelson & Nelson 2016; Hamblen & Henderson 2020a,b, 2022). Additionally, sea ice  
70 influences oxygen and methane dynamics through abiotic and biotic processes (Tison et al 2016) and strongly  
71 influences marine plankton - which I propose may dominate the seasonal oxygen cycle and contribute to the carbon  
72 dioxide cycle (Hamblen 2022). In contrast, argon dynamics will be only indirectly influenced by the biota  
73 (potentially through effects on climate, Hamblen 2017), making it an inert tracer for some processes.

74

75 In this study I examine data on atmospheric argon from a global monitoring program (Scripps O<sub>2</sub> Program, 2022). I  
76 address the question: do seasonal cycles of atmospheric argon vary closely with those of sea ice extent? Given the  
77 behaviours of carbon dioxide, oxygen and methane (Hamblen & Henderson 2020a,b, 2022), I predict the local  
78 seasonal cycle of argon will usually be pronounced (high amplitude and clear) where that of carbon dioxide is  
79 pronounced, particularly the Northern Hemisphere high-latitude recording sites. I predict Greenland Sea sea ice  
80 extent will have high phenological similarity with argon phenology because it does with carbon dioxide (Hamblen &  
81 Henderson 2020a, 2022).

82

83

## 84 **Methods**

### 85 *Datasets*

86 I use the datasets in Table 1.

87

88

89 **Table 1** Data sources

Variable	Source
Atmospheric argon ( <sup>40</sup> Ar)  Monthly average	Scripps O <sub>2</sub> Program <a href="https://scripps2.ucsd.edu/index.html">https://scripps2.ucsd.edu/index.html</a> <a href="https://scripps2.ucsd.edu/data.html">https://scripps2.ucsd.edu/data.html</a>  Argon to nitrogen ratio: Ar / N <sub>2</sub> described by Scripps as "the 40 concentration in ppm units".  'Monthly average' flask data.  Accessed 10 October 2022.
Sea ice extent, Arctic and Antarctic	<a href="https://nsidc.org/data/seaice_index/archives">https://nsidc.org/data/seaice_index/archives</a> Sea Ice Index Version 3 <a href="ftp://sidads.colorado.edu/DATASETS/NOAA/G02135/">ftp://sidads.colorado.edu/DATASETS/NOAA/G02135/</a>  (Fetterer et al 2017)  'North' (= 'Arctic'): <a href="ftp://sidads.colorado.edu/DATASETS/NOAA/G02135/north/monthly/data/">ftp://sidads.colorado.edu/DATASETS/NOAA/G02135/north/monthly/data/</a> at <a href="http://sidads.colorado.edu">sidads.colorado.edu</a>  'South' (= 'Antarctic'): <a href="ftp://sidads.colorado.edu/DATASETS/NOAA/G02135/south/monthly/data/">ftp://sidads.colorado.edu/DATASETS/NOAA/G02135/south/monthly/data/</a>  Files in form: S_01_extent_v3.0.csv.  Accessed 19 February 2022.
Sea ice extent, Greenland Sea	<a href="ftp://sidads.colorado.edu/DATASETS/NOAA/G02186/">ftp://sidads.colorado.edu/DATASETS/NOAA/G02186/</a> MASIE NSIDC/NIC Sea Ice Product G02186 - Daily Ice Extent by Region in Square Kilometers.  National Ice Center and National Snow and Ice Data Center. Compiled by F. Fetterer, M. Savoie, S. Helfrich, and P. Clemente-Colón. 2010, updated daily. Multisensor Analyzed Sea Ice Extent - Northern Hemisphere (MASIE-NH), Version 1. Subset: 4km. Boulder, Colorado USA. NSIDC: National Snow and Ice Data Center. doi: <a href="https://doi.org/10.7265/N5GT5K3K">https://doi.org/10.7265/N5GT5K3K</a>  Accessed 22 February 2022.
Atmospheric carbon dioxide  Monthly average	<a href="https://www.esrl.noaa.gov/gmd/dv/data/">https://www.esrl.noaa.gov/gmd/dv/data/</a>  Lan et al (2022).  Accessed 16 October 2022.

90

91

92 ***Atmospheric sampling locations***

93 Atmospheric argon levels are routinely monitored at ten recording stations, simultaneously with those of carbon  
94 dioxide and oxygen, as part of a study of global oxygen dynamics (Scripps O<sub>2</sub> Program 2022). These cover a range  
95 of latitudes but have very little replication within latitudes. Two other recording sites in the Scripps O<sub>2</sub> Program with  
96 no data after 2006 (when the sea ice data start) were examined briefly but are not included here since nothing  
97 exceptional is evident in their very short time-series (Hambler unpublished). Data for argon levels are available from  
98 the Scripps O<sub>2</sub> Program as the Ar / N<sub>2</sub> ratio; the values are given by Scripps in "ppm units" (parts per million)  
99 although values are a ratio, compared to a reference, and include negative values. For simplicity this variable is  
100 hereafter abbreviated to 'argon'.

101 As in previous studies of gas dynamics and sea ice, I consider rates of change of atmospheric gases more informative  
102 for the purposes of identifying flux locations than are the raw data on the levels of these gases (Hamblar &  
103 Henderson 2020a, 2022; Hamblar 2022). A 'monthly average' data set is available for argon from the Scripps O<sub>2</sub>  
104 Program and is used here for ease of comparison with monthly sea ice and carbon dioxide data, although some fine  
105 detail of the gas cycles may be lost in the averaging and other processing (Hamblar & Henderson 2020a; Hamblar  
106 2022). 'Monthly' rates of change of gas are derived from extent in month two minus extent in month one, plotted in  
107 month two.

108

109 Data for carbon dioxide flask sample monthly average values are available from the National Oceanic and  
110 Atmospheric Administration (NOAA) Global Monitoring Laboratory (GML) Carbon Cycle Greenhouse Gases (Lan  
111 et al 2022).

112

### 113 *Sea ice*

114 Sea ice extent data were chosen to be directly comparable with previous work on carbon dioxide, methane and  
115 oxygen dynamics (Hamblar & Henderson 2020a,b, 2022; Hamblar 2022). For 'Arctic' and 'Antarctic' sea ice extents  
116 I use data from National Snow and Ice Data Center (NSIDC) for the 'North' and 'South'. For a 'global' sea ice  
117 monthly extent I sum Arctic and Antarctic monthly extents, as per Hamblar & Henderson (2022). I also use sea ice  
118 extent for the 'Greenland Sea', a sub-region for the Arctic previously found to have particularly high statistical  
119 correlation with carbon dioxide flux (Hamblar & Henderson 2020a) and to have high visual similarity with oxygen  
120 flux (Hamblar 2022). These data were obtained from MASIE at 4 km resolution for the Greenland Sea (mapped at  
121 <ftp://sidacs.colorado.edu/DATASETS/NOAA/G02186/>). Sea ice extent rate is measured in square kilometres per  
122 month. Rates of change of ice are derived from extent in month two minus extent in month one, plotted in month  
123 two.

124

### 125 *Time-series durations, gaps and lags*

126 For ease of comparison I choose time-series durations similar to those used in previous research on carbon dioxide  
127 and sea ice (Hamblar & Henderson 2020a, 2022; Hamblar 2022). Sea ice extent data with presumed consistent  
128 methodology are readily available from early 2006. Even such short time-series are sufficient to reveal very strong  
129 correlations (Hamblar & Henderson 2020a,b, 2022). Strong visual similarity of seasonal phenologies of sea ice and  
130 carbon dioxide rates invariably reflects very high statistical correlation (Hamblar & Henderson 2020a,b, 2022).  
131 Statistical analyses are not performed here due to the complexities of missing data points; however, only strong  
132 patterns are likely to be detectable visually. Since many high-latitude phenomena are likely to be correlated, it is the  
133 fine detail of the multiple spikes on the seasonal curves, rather than the overall correlation, that is potentially of  
134 greatest interest; however, this detail will be hard to analyse formally so I hope others will build on this work and  
135 test for more subtle patterns.

136

137 Previous work has found the strongest correlations between time-series and the strongest visual similarities can  
138 involve lags between the series (Hamblar & Henderson 2020a,b, 2022; Hamblar 2022); visually aligning the most  
139 extreme rates in the cycles is particularly helpful in identifying the lag. The Mauna Loa gas rate often lags about one  
140 month behind northern high-latitude sites, and about seven months behind southern high-latitude sites. The South  
141 Pole gas rate often lags about a month behind coastal Antarctic and Southern Ocean sites. These lags are possibly  
142 due to delays in gases moving between latitudes and altitudes. In the results for argon these lag durations established  
143 for carbon dioxide are used for the seasonal curves presented in the relevant Figures, although some slightly shorter  
144 or longer lags were explored and produced no substantially stronger visual fits between time-series (Hamblar  
145 unpublished).

146

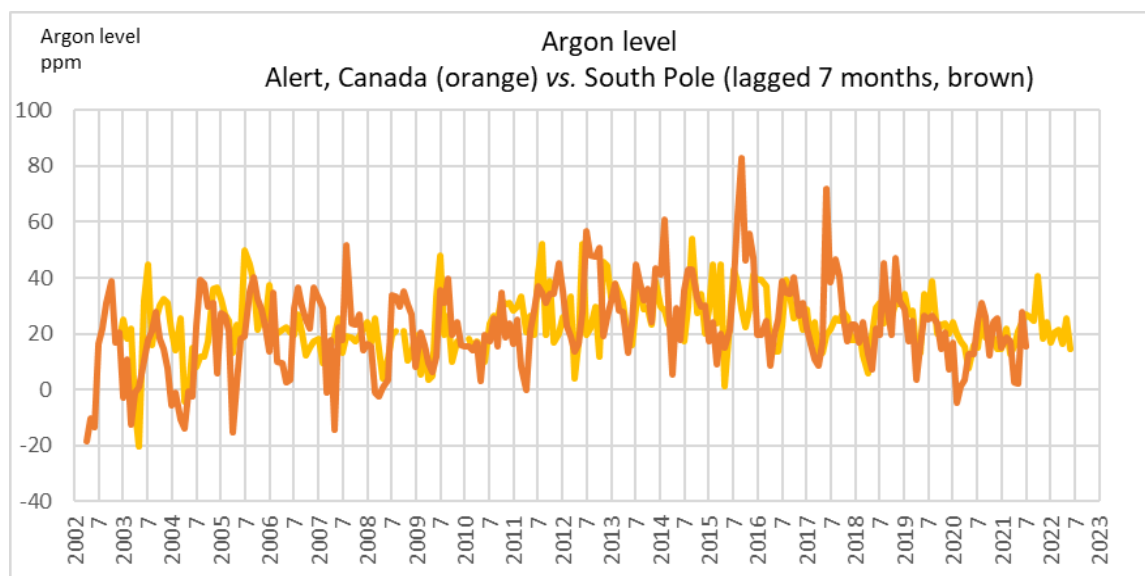
147 In some Figures (as indicated in the captions) the highest and lowest values of the gas rate are not displayed in the  
 148 range included on the y-axis, because to include them would obscure the detail of the curves near the zero value on  
 149 the axis. Such outliers are not essential to reveal some patterns but would have value for future studies of  
 150 mechanisms, and some outliers are artefacts (Cassar et al 2008).

151

152 **Results**

153 Seasonal cycles of the argon level at Alert (Canada), the South Pole and Mauna Loa (Hawaii) are shown in Figs. 1  
 154 and 2, illustrating the two most high-latitude sites and a tropical site often considered globally typical of carbon  
 155 dioxide levels (Ciais et al 2013).

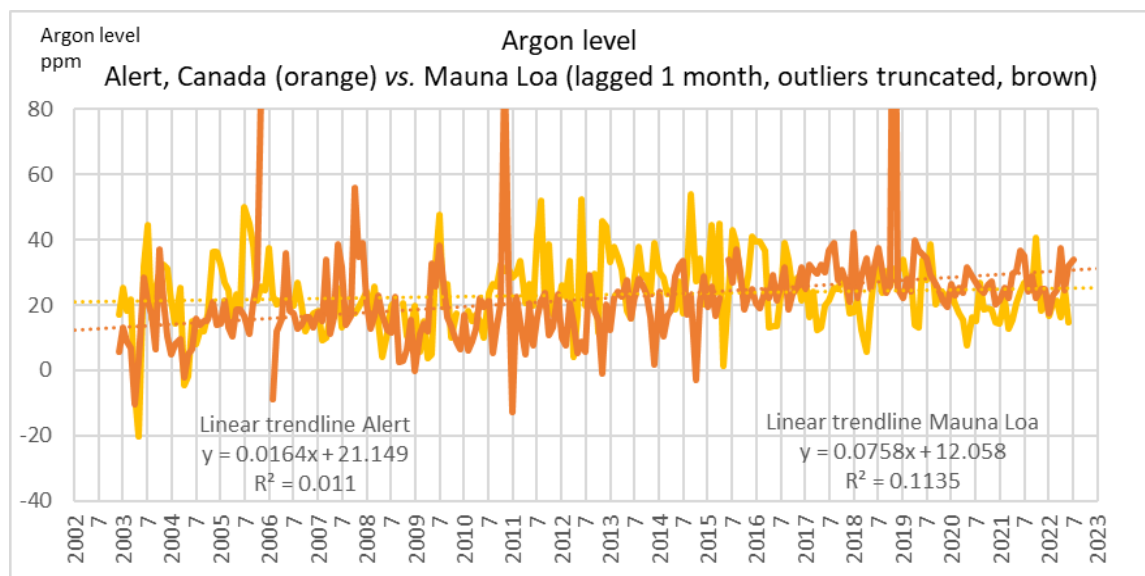
156



157

158 **Fig. 1** Levels of atmospheric argon at Alert (Canada) and the South Pole (lagged 7 months).

159



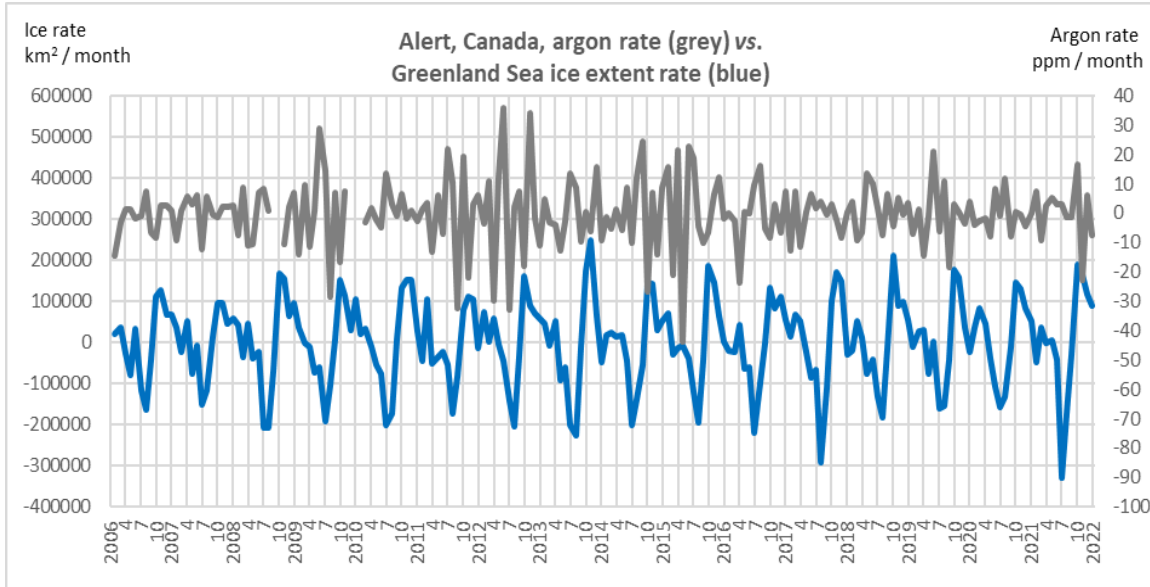
160

161 **Fig. 2** Levels of atmospheric argon at Alert (Canada) and Mauna Loa (Hawaii) (lagged 1 month). Note outliers are  
 162 cut off to enable easier comparison of the fine detail. Linear trendlines include outliers.

163

164 Rates of change of argon and sea ice are most easily compared visually, as in Figs. 3 - 14. Sites are listed from north  
165 to south, and the latitude and longitude of the recording station is given in the captions.

166

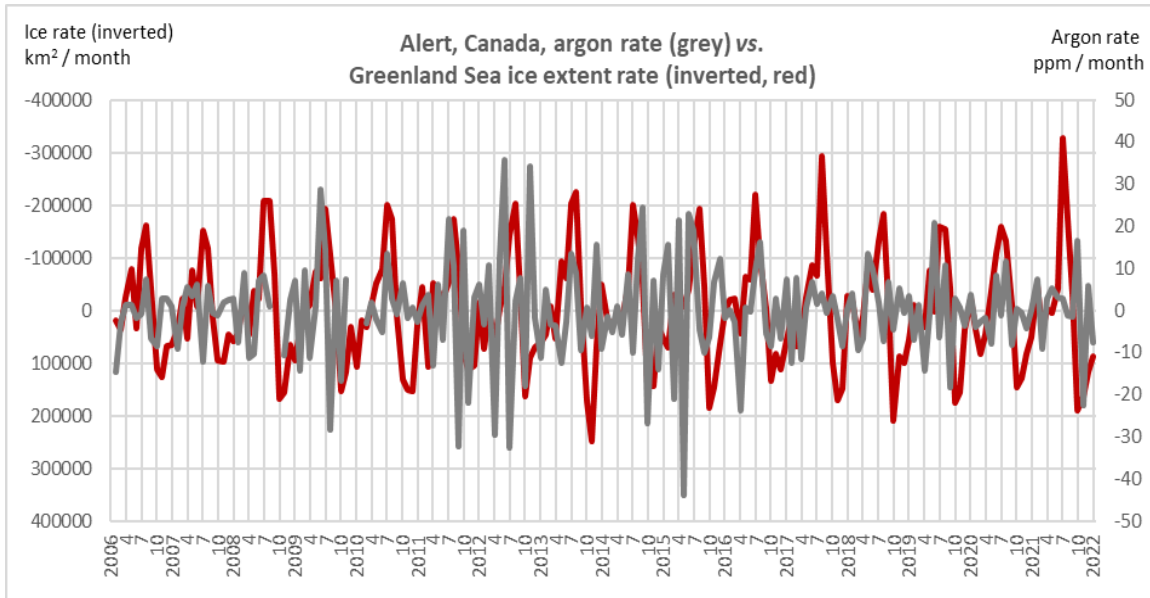


167

168 **Fig. 3** Comparison of Greenland Sea sea ice extent rate and argon rate, Alert, Canada (82N, 62W). Zeros on axes  
169 are not aligned. Note the 'Greenland -type Phenology' (GTP) of the sea ice including a sawtooth as the rate of ice  
170 extension declines and becomes negative.

171

172

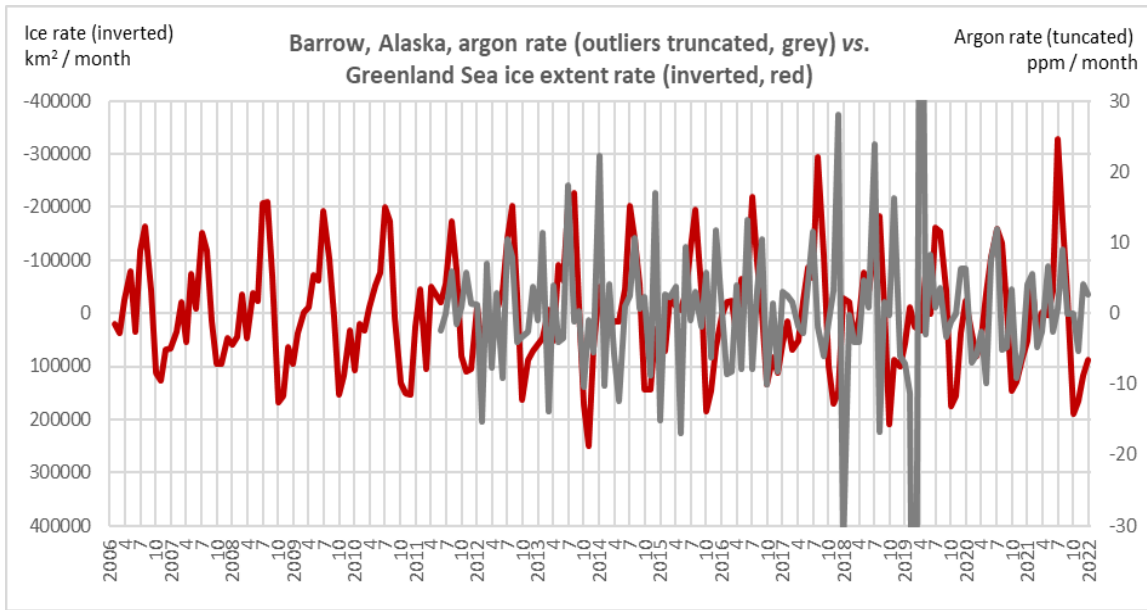


173

174 **Fig. 4** Comparison of Greenland Sea sea ice extent rate (inverted axis) and argon rate, Alert, Canada (82N, 62W).  
175 Note scale for argon differs to that in Fig. 3.

176

177



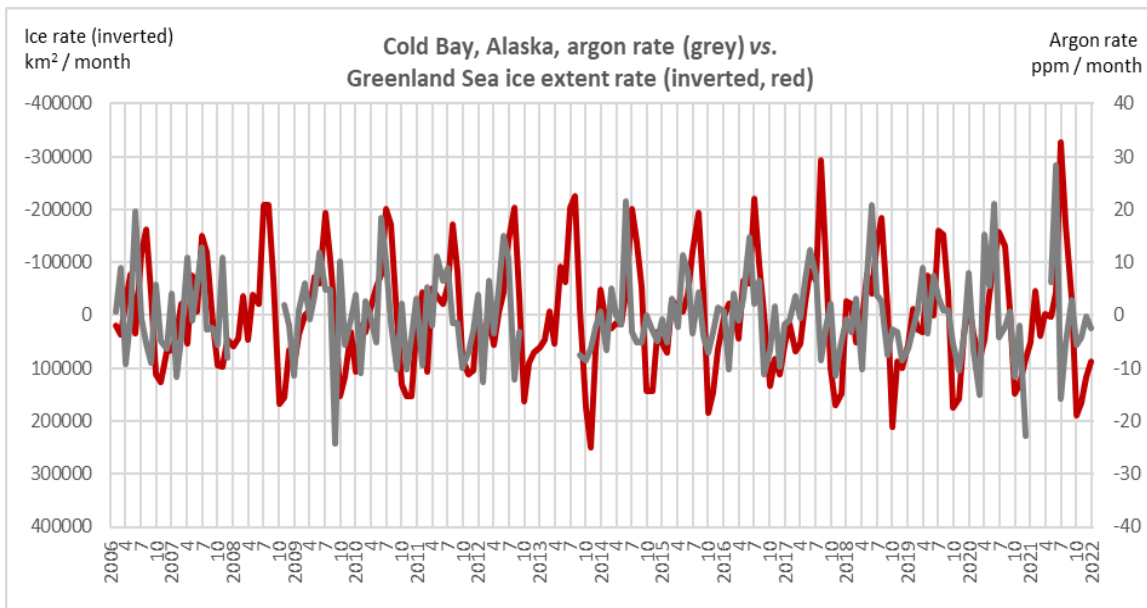
178

179 **Fig. 5** Comparison of Greenland Sea sea ice extent rate (inverted axis) and argon rate, Point Barrow, Alaska (71N,  
180 157W). Outlier values cut off.

181

182

183

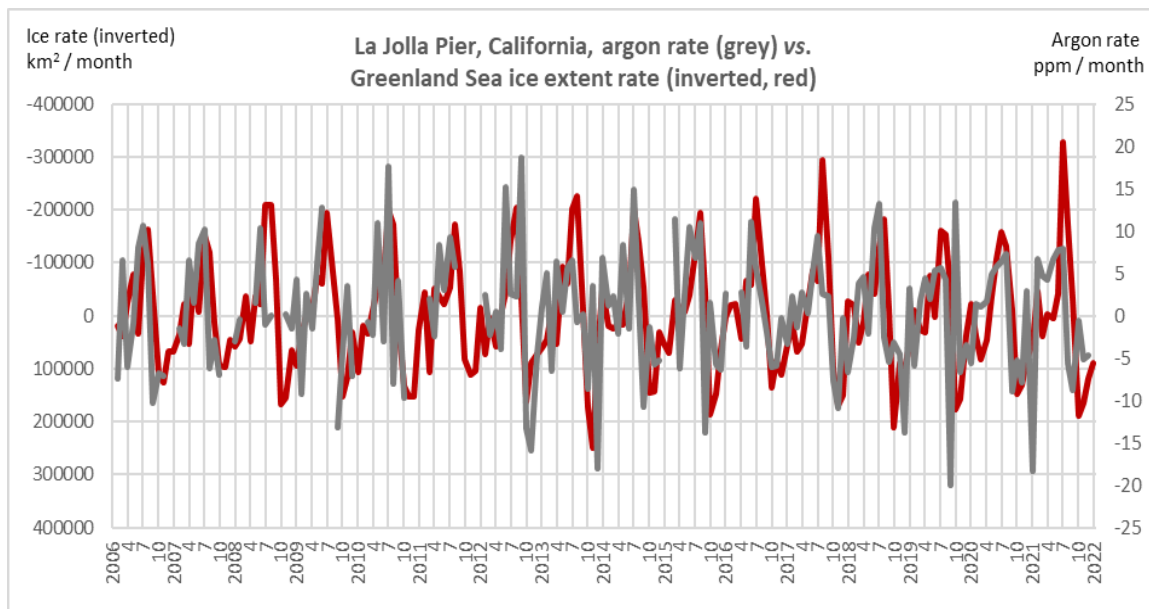


184

185 **Fig. 6** Comparison of Greenland Sea sea ice extent rate (inverted axis) and argon rate, Cold Bay, Alaska (55N,  
186 163W).

187

188

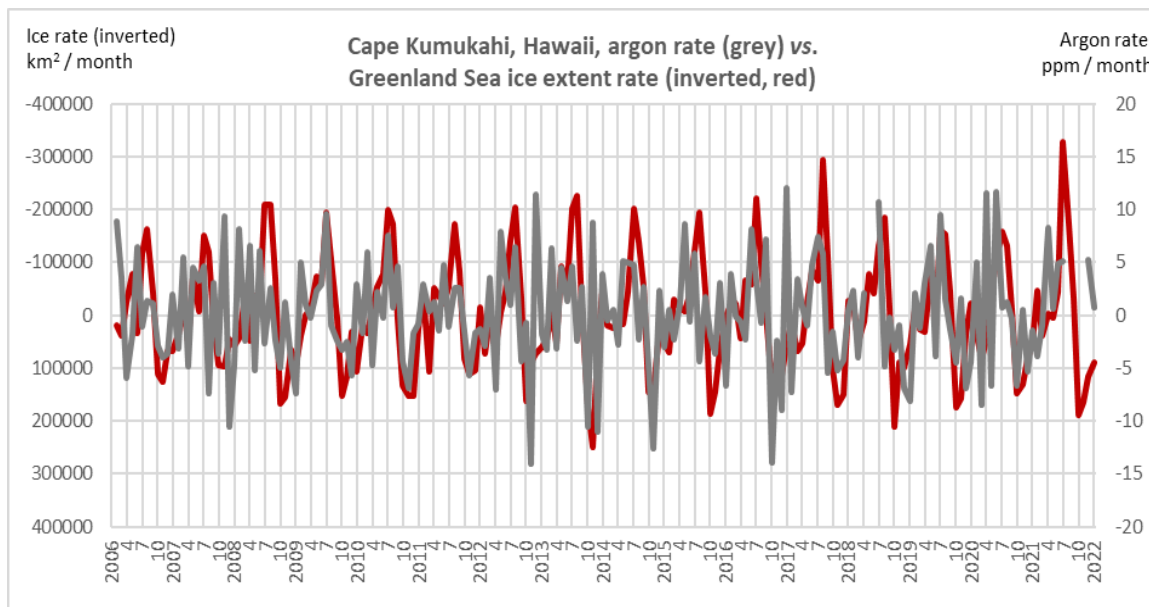


189  
190 **Fig. 7** Comparison of Greenland Sea ice extent rate (inverted axis) and argon rate, La Jolla Pier, California (33N,  
191 117W).

192

193

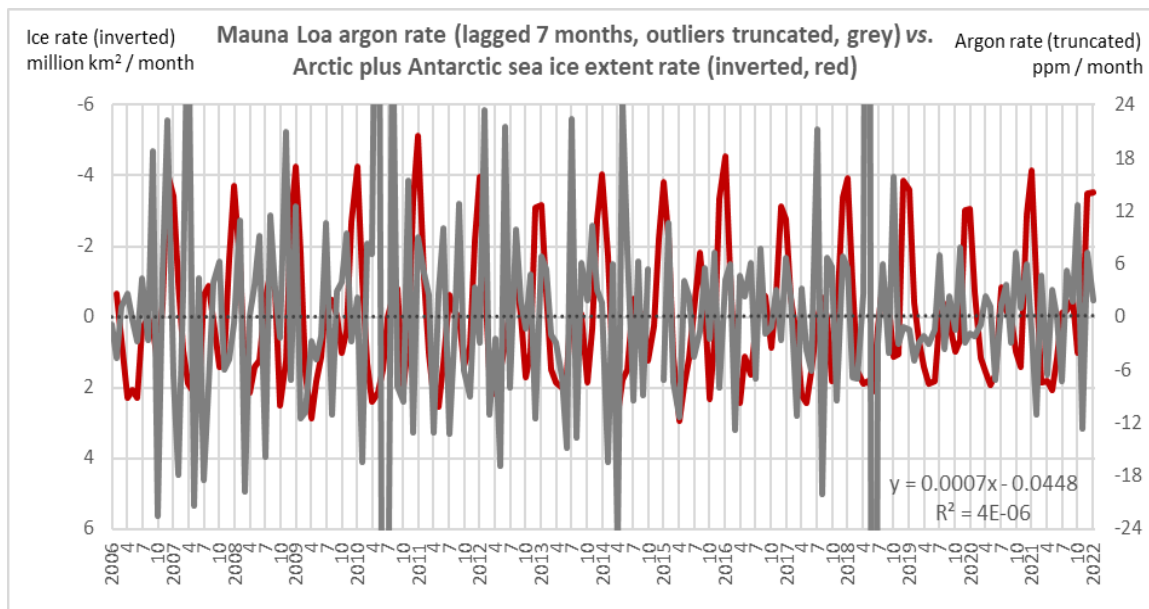
194



195  
196 **Fig. 8** Comparison of Greenland Sea sea ice extent rate (inverted axis) and argon rate, Cape Kumukahi, Hawaii  
197 (19.5N, 155W).

198

199

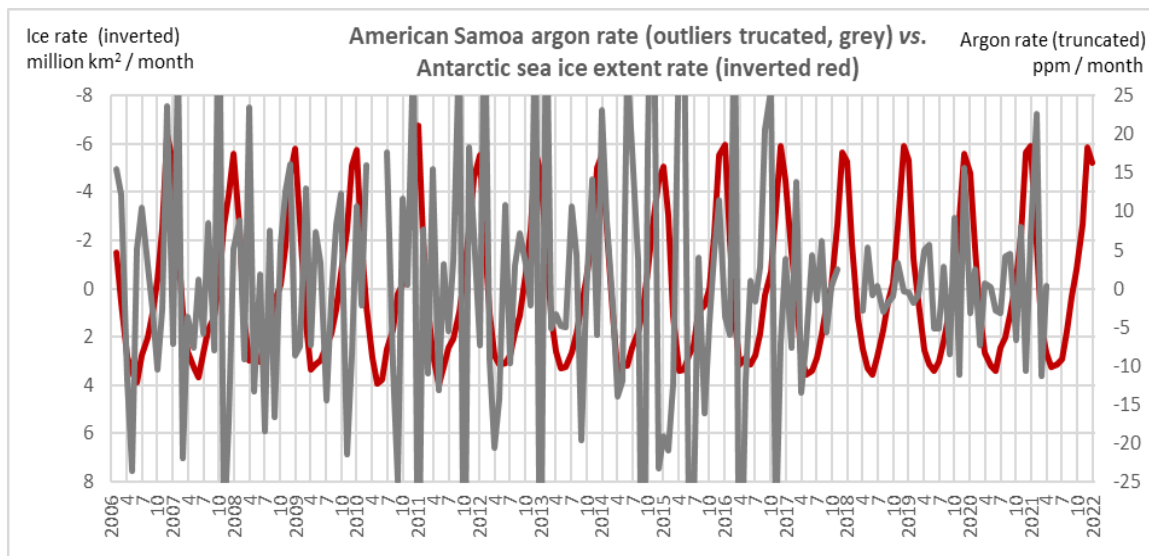


200  
 201 **Fig. 9** Comparison of 'Arctic plus Antarctic' sea ice extent rate (inverted axis) and argon rate, Mauna Loa, Hawaii  
 202 (19.5N, 156W). Argon rate lagged 7 months. Outlier values cut off. Note linear trendline for argon (grey dots).

203

204

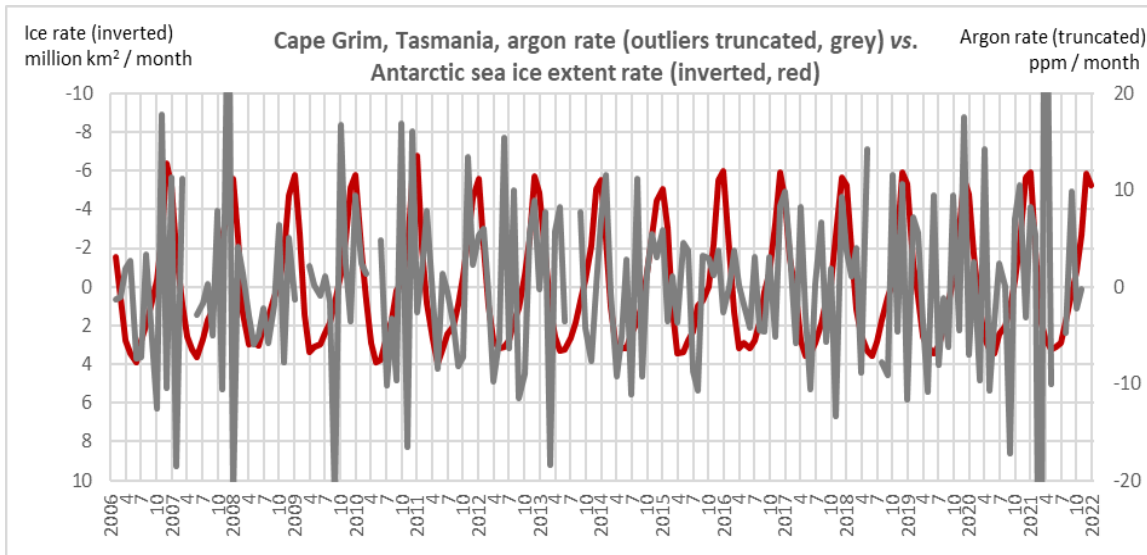
205



206  
 207 **Fig. 10** Comparison of Antarctic sea ice extent rate (inverted axis) and argon rate, American Samoa, Pacific Ocean  
 208 (14.5S, 170W). Outlier values cut off.

209

210

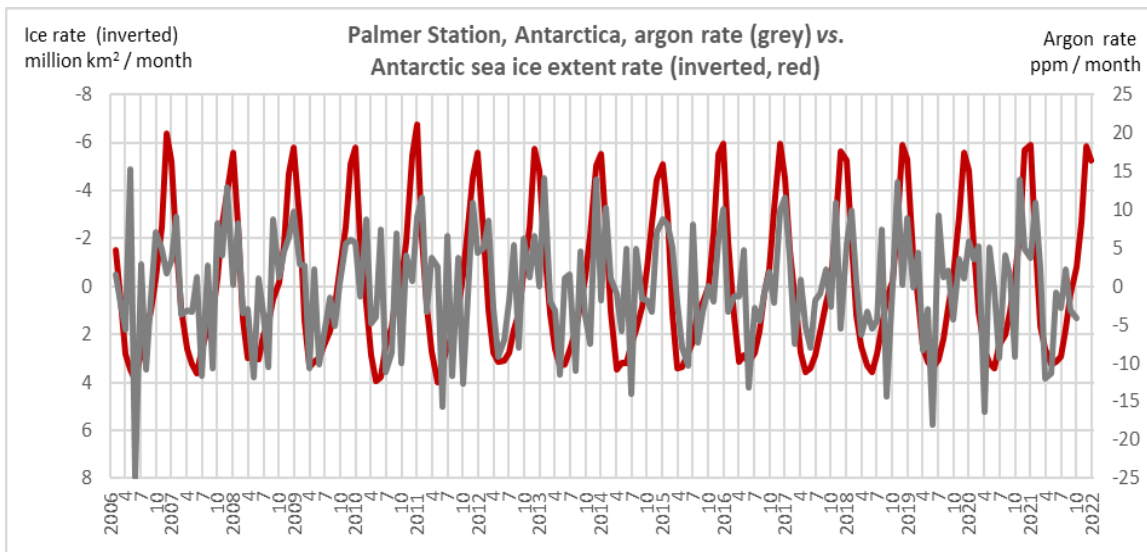


211  
212 **Fig. 11** Comparison of Antarctic sea ice extent rate (inverted axis) and argon rate, Cape Grim, Tasmania (41S,  
213 150E).

214

215

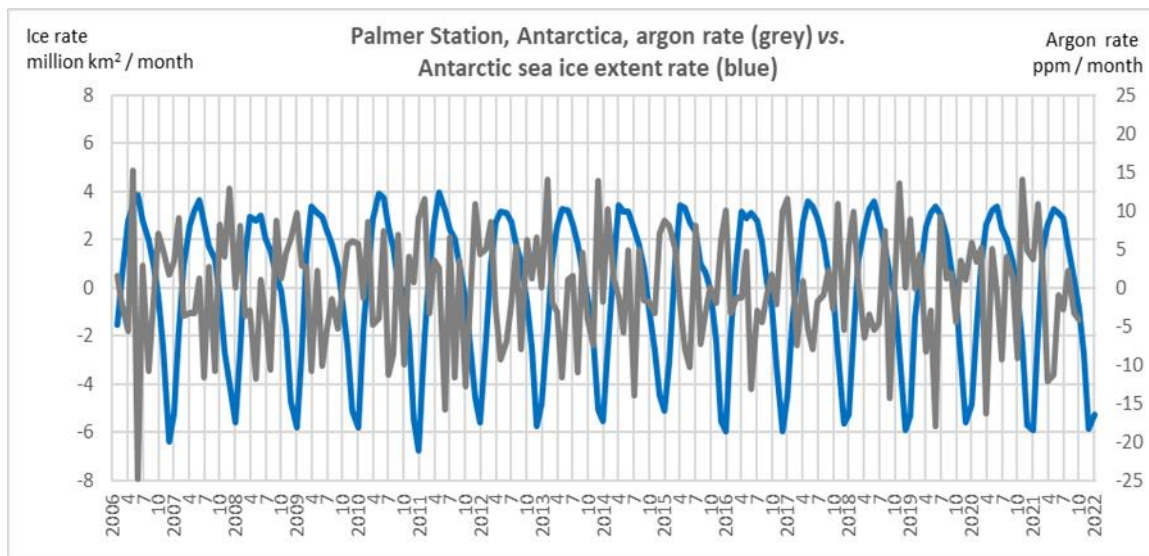
216



217  
218 **Fig. 12** Comparison of Antarctic sea ice extent rate (inverted axis) and argon rate, Palmer Station, Antarctic  
219 Peninsula (65S, 64W).

220

221

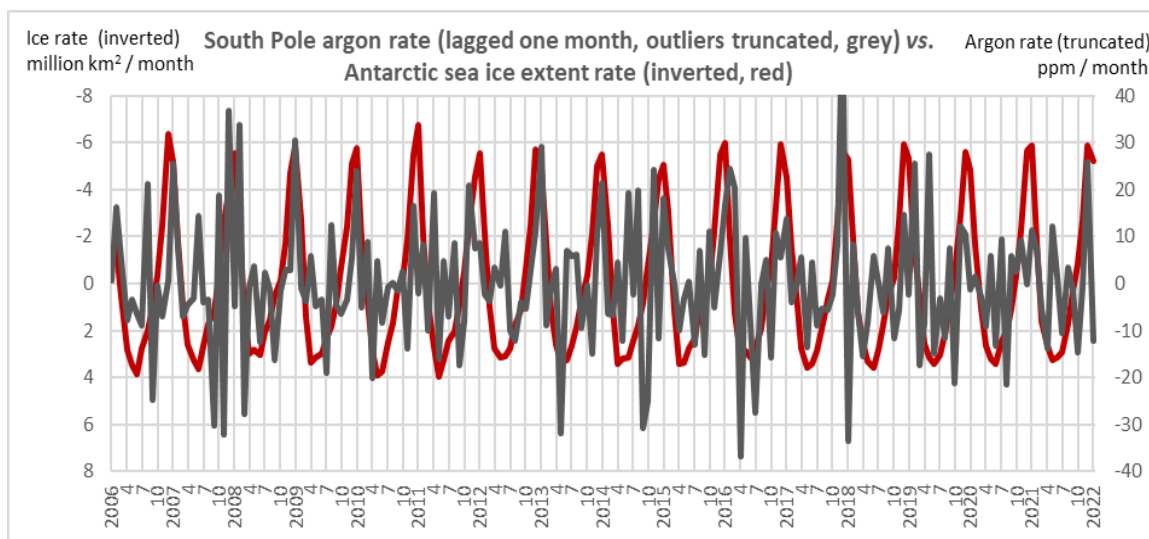


222

223 **Fig. 13** Comparison of Antarctic sea ice extent rate and argon rate, Palmer Station, Antarctic Peninsula (65S, 64W).  
 224 Data as in Fig. 11 but ice rate axis not inverted.

225

226



227

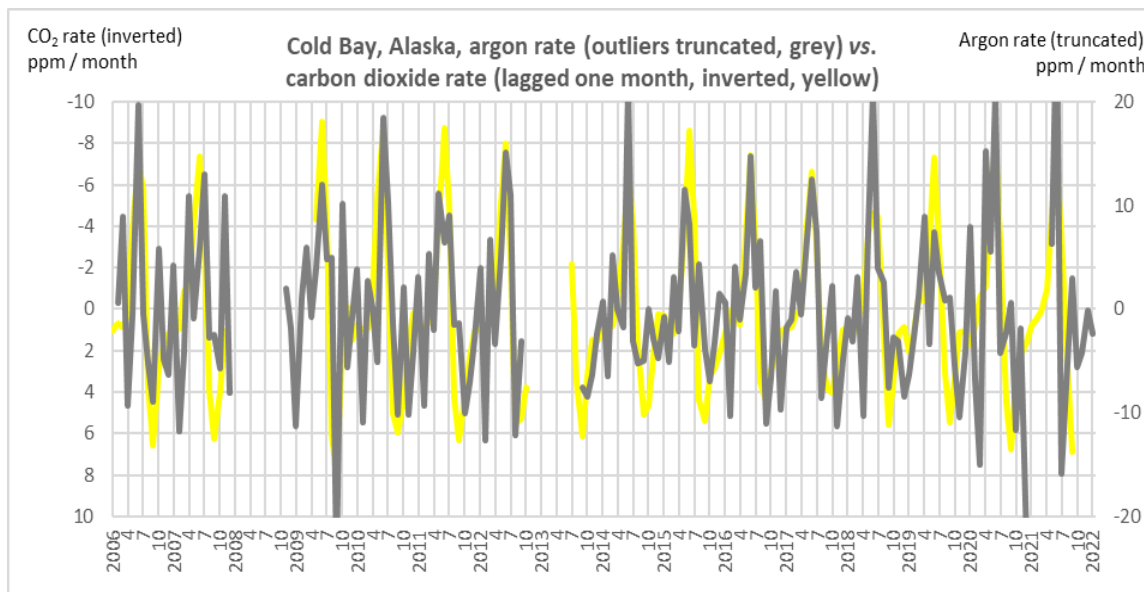
228 **Fig. 14** Comparison of Antarctic sea ice extent rate (inverted axis) and argon rate, South Pole (90S, 0E). Argon rate  
 229 lagged one month.

230

231

232 Comparisons between argon rate and carbon dioxide rate are given in Figs. 15 and 16. These two high-latitude sites  
 233 are selected visually on the basis of relatively low 'noise' in the argon rate.

234

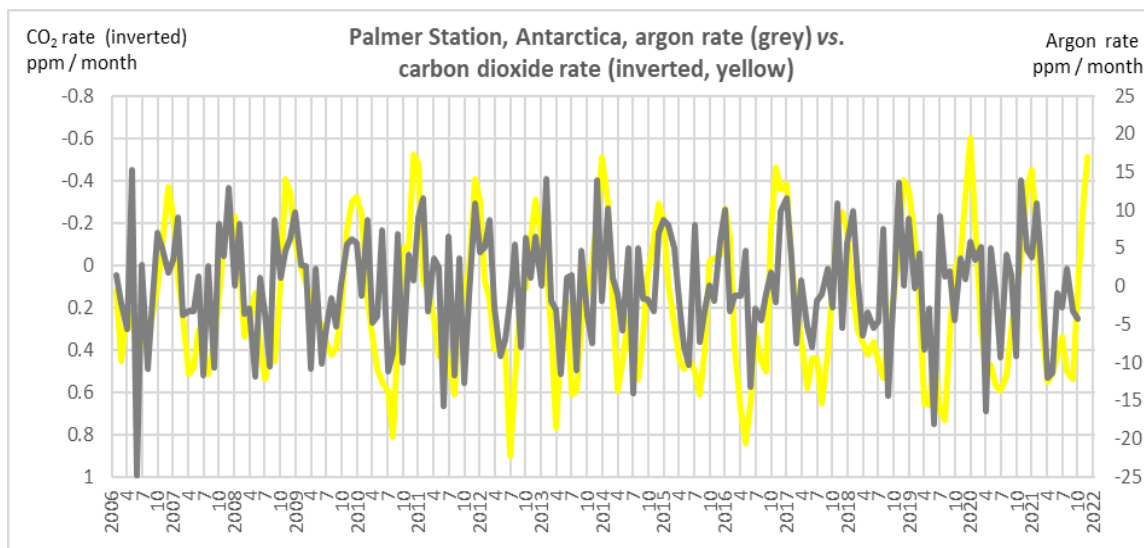


235

236 **Fig. 15** Comparison of argon rate and carbon dioxide rate (inverted axis), Cold Bay, Alaska (55N, 163W). Carbon  
 237 dioxide rate lagged one month.

238

239



240

241 **Fig. 16** Comparison of argon rate and carbon dioxide rate (inverted axis), Palmer Station, Antarctic Peninsula (65S,  
 242 64W).

243

244 **Discussion**

245 The seasonal cycles in the argon rate are generally far less visually obvious than for carbon dioxide rate or methane  
 246 rate at the recording sites where all these gases can be compared (Hambler & Henderson 2020a,b). Argon has a  
 247 much 'noisier' cycle with peaks in rates at more frequent (and visually erratic) intervals, and often very sharp spikes  
 248 (e.g. the 'outliers' in Figs. 2 and 9). It is not clear if some outliers are a result of local conditions or instrumentation  
 249 or other technical issues (Battle et al 2003; Cassar et al 2008) but it is interesting that a sharp argon increase occurs  
 250 when there is a sharp drop in oxygen at Mauna Loa in 2018 (Fig. 2, and Figure 1 in Hambler 2022). Sporadic events  
 251 such as arrival of pockets of air (Cassar et al 2008) and oceanic upwelling of water at different argon saturation  
 252 levels (Hamme & Emmerson 2002; Ito & Deutsch 2006; Ito et al 2011) might be responsible for some spikes. I

253 hypothesize wind-associated injection of bubbles into water (Stanley et al 2009) or rainfall might be relevant to some  
254 spikes.

255

256 Consistent with work at Barrow, and studies of tanks and models (Zhou et al 2013; Moreau et al 2014), atmospheric  
257 argon growth rates often have strong peaks at times of peak sea ice melt within a Hemisphere (Figs. 3 - 14). Unlike  
258 for carbon dioxide or methane (Hamblar & Henderson 2022) there are often multiple strong spikes of atmospheric  
259 argon increase between the annual spring peaks, and these may have faster rates of increase or decrease than the  
260 more regular peaks. Rapid release of argon bubbles to the atmosphere might be expected from around May and June  
261 at Barrow (Zhou et al 2013; Moreau et al 2014) and observed peaks of net emission rate at Barrow and other  
262 northern high-latitude sites often occur around July (Figs. 3 - 6) although many may be coincidences.

263

264 The high-latitude sites (Alert, Barrow, Cold Bay, Cape Grim, Palmer and the South Pole, Figs. 4 - 6, 11 - 14) show  
265 the clearest similarity to sea ice rates, as is the case with carbon dioxide, methane and oxygen (Hamblar &  
266 Henderson 2020a, 2022; Hamblar 2022) which may suggest sea ice is either a driver of the gas dynamics or is very  
267 strongly correlated with an as yet unidentified high-latitude driver. Greater amplitudes of sea temperature change at  
268 high latitudes is arguably sufficient to explain this general pattern (Cassar et al 2008). However, fine details of the  
269 gas cycles are consistent with sea ice being a potential driver but would be harder to explain through sea temperature  
270 alone.

271

272 Notably, with an inverted axis for ice (Figs. 4 - 8), northern high-latitude sites show a weak visual similarity to the  
273 'Greenland-type Phenology' identified for carbon dioxide (Hamblar & Henderson 2020) where the fine detail of the  
274 winter variation in the Greenland Sea ice growth is often matched in the fine detail of the gas dynamics. Sea  
275 temperature and sea ice near Greenland show complex dynamics (Shuchman et al 1998; Kawasaki & Hasumi 2016)  
276 which may generate this signature. At Alert, Barrow, Cold Bay and La Jolla Pier some argon peaks occur in close  
277 synchrony with minor peaks in winter ice growth in the Greenland Sea, but with a less good fit of magnitudes than  
278 for carbon dioxide (Hamblar & Henderson 2020a). Even the tropical Cape Kumukahi (Hawaii) has a sawtooth  
279 pattern with some similarity to the winter spikes of Greenland Sea ice extension (Fig. 8). Although the timings of  
280 peak argon rates at these sites are often synchronous with maximum positive or negative Greenland Sea ice rates, the  
281 peaks for argon are less similar in amplitude to the sea ice peaks than are those of carbon dioxide or methane  
282 (Hamblar & Henderson 2020a) and would require detailed analysis to test for significance.

283

284 The high-latitude southern sites (Cape Grim, Palmer and the South Pole, Figs. 11 - 14) show seasonality similar to  
285 the Antarctic sea ice, again with substantial 'noise' of intermittent peaks compared to the very close fit of carbon  
286 dioxide or methane (Hamblar & Henderson 2020a,b, 2022). As with carbon dioxide, the South Pole argon rate lags  
287 the rate at Cape Grim and Palmer by about a month, consistent with a putative transport lag from a marine source of  
288 the pattern.

289

290 Unlike for carbon dioxide, methane or oxygen, Mauna Loa does not have an easily recognized Greenland-type  
291 Phenology for argon. Nor is its argon rate phenology very similar to the combined rate of change of 'Arctic plus  
292 Antarctic' sea ice (Fig. 9). At Mauna Loa, carbon dioxide, methane and oxygen seasonal cycles often have a twin-  
293 peak (Hamblar & Henderson 2022; Hamblar 2022) not obvious for argon. From visual inspection I argue there is a  
294 weak coherence between the gas and ice rates at Mauna Loa which would merit formal investigation. It is possible  
295 there are local and intense 'deliveries' of argon to Mauna Loa that mask signals from the Arctic or Antarctic. If  
296 confirmed statistically, a lag of argon rates at Mauna Loa about seven months behind sea ice rates would support the  
297 regional origins of the major fluxes of argon and carbon dioxide being similar (and at high-latitudes).

298

299 American Samoa has very complex and relatively erratic argon dynamics (Fig. 10) with at times a relatively high rate  
300 of change and level of argon, and is also distinctive for oxygen (Manning et al 2003; Hambler 2022). Some  
301 synchrony of peak Antarctic sea ice melt and argon increase is visible in Fig. 10 but there are many other peaks in  
302 argon rates. Only a small seasonal signal is expected from outgassing at this site due to low temperature variation in  
303 the tropical ocean (Cassar et al 2008). Again, potential local 'sources' and 'sinks' of water and air with different argon  
304 levels should be investigated.

305

306 There are few sampling sites for argon, and several display highly variable monthly rates of change, so it is not  
307 possible to make strong conclusions about relative amplitudes of the argon rate cycles at different latitudes (as with  
308 argon levels, Cassar et al 2008). Based on the seasonal cycles of carbon dioxide, methane and oxygen (Hambler &  
309 Henderson 2022; Hambler 2022) I predict further sampling would reveal generally high amplitudes of rates of  
310 change of argon at both northern and southern high latitudes, and that each Hemisphere has a very large air mass  
311 with similar abundance and phenology of argon at high latitudes. Indeed, Cassar et al (2008) found all five of their  
312 Southern Hemisphere sites to be in phase, with lower amplitudes in argon levels in the tropics.

313

314 If sea ice extent is not a driver in the argon cycle, it is a proxy for a large-scale phenomenon that does; in the  
315 Northern Hemisphere this driver would have similar fine details to the Greenland Sea ice extent rate. Candidates  
316 include combinations of temperature, wind speed and direction (*e.g.* Shuchman et al 1998), ocean currents, vertical  
317 mixing and ocean ventilation.

318

319 The peak in atmospheric argon increase within a Hemisphere when ice melts has similar timing to the peak net  
320 emission of oxygen (Hambler 2022) but is in antiphase with carbon dioxide and methane (Hambler & Henderson  
321 2020a,b, 2022). For two sites selected here because they have relatively clear seasonal argon cycles (Cold Bay,  
322 Alaska, and Palmer Station, Antarctica) the cycles of carbon dioxide and argon can be more easily compared (Figs.  
323 15 - 16). The very pronounced peak drop in high-latitude atmospheric carbon dioxide during peak sea ice melt often  
324 coincides with a peak in growth in atmospheric argon. This difference between the gases in summer could be partly  
325 due to more argon escaping in bubbles than being absorbed into cold meltwater. The difference may also be due to  
326 processes which do not influence argon - such as photosynthetic uptake of carbon dioxide and calcium carbonate  
327 dissolution in spring which draws down carbon dioxide from the atmosphere (Vancoppenolle et al 2013; Hambler &  
328 Henderson 2020a, 2022; Hambler 2022). Freeze-degassing sea water drives some argon into bubbles trapped in the  
329 ice (Moreau et al 2014) whilst some carbon dioxide is released to the atmosphere during the precipitation of calcium  
330 carbonate (ikaite) crystals in growing ice (Rysgaard et al 2007; Dieckmann et al 2010; Geilfus et al 2013;  
331 Vancoppenolle et al 2013). Small winter extensions of sea ice near Greenland might thus cause decreased argon  
332 emission to the atmosphere but increased carbon dioxide emission.

333

334 As with carbon dioxide and oxygen rates (Hambler & Henderson 2022; Hambler 2022) the time-series in the argon  
335 level or rate from 2006 show no strong trend (*e.g.* linear trendlines in Figs. 2, 9); however, long timeseries with less  
336 noise would be required to detect a signal from ocean warming and associated outgassing (Cassar et al 2008). El  
337 Niño cycles are associated with argon emission rates (Ito et al 2011) as with carbon dioxide (Salby 2012; Hambler &  
338 Henderson 2020a). A low decadal trend would be consistent with outgassing from massive volumes of slowly  
339 warming sea water.

340

341

342

343

## 344 **Conclusions**

345 Seasonal patterns of change of argon have similarities to sea ice extent within each hemisphere, but show less  
346 coherence than do carbon dioxide, methane and oxygen - suggesting multiple drivers of atmospheric argon dynamics  
347 despite it being a noble gas. If sea ice is a driver of argon exchange, as fieldwork, tank experiments, modelling and  
348 visual comparison of patterns suggest it could be, then seasonal dynamics of other gases such as carbon dioxide  
349 should be reviewed to test for a related abiotic mechanism. Abiotic exchanges of argon between sea, sea ice and  
350 atmosphere may indicate pathways that may be shared by some other gases but which have been under-sampled and  
351 under-appreciated. There are abiotic processes with magnitudes distinctive to each gas (such as bubble formation in  
352 sea ice, or calcium carbonate dissolution) which could contribute to differences in seasonal cycles of argon, carbon  
353 dioxide, methane and oxygen.

354

355 I suggest that through degassing and 'amplification' processes, sea ice may cause more intermittent and sharp changes  
356 in gas rates than occur more widely in sea water through temperature-dependent solubility changes. Annual large-  
357 scale weather patterns driving sea ice extensions near Greenland should be investigated as possible contributors to  
358 argon and other gas dynamics. Detailed statistical examination is required to test the weaker visual similarities or  
359 apparent lack of relationships between time-series reported here. The importance of further painstaking research in  
360 the very challenging high-latitude regions is well illustrated by argon.

361

## 362 **Declarations**

363 *Funding* None.

364 *Conflict of interest / Competing interest* The author declares he has no conflict of interest / competing interests.

365 *Availability of data and material* Data are available online from the sources indicated in the Methods.

366 *Code availability* Not applicable.

367

## 368 **Open Access**

369 This article is distributed under the terms of the Creative Commons Attribution 4.0 International License  
370 (<http://creativecommons.org/licenses/by/4.0/>), which permits unrestricted use, distribution, and reproduction in any  
371 medium, provided you give appropriate credit to the original author(s) and the source, provide a link to the Creative  
372 Commons license, and indicate if changes were made.

373

## 374 **Acknowledgements**

375 Datasets in Table 1 are the work of remarkable efforts over many years by individuals and organisations including:  
376 National Snow and Ice Data Center (NSIDC); Scripps Institution of Oceanography; Scripps O<sub>2</sub> Program. I thank all  
377 sources listed or indicated in the metadata on the hosting websites and in Table 1, including the National Science  
378 Foundation USA and U.S. National Weather Service.

379

## 380 **References**

- 381 Angelopoulos, M., Damm, E., Simões Pereira, P. et al (2022) Deciphering the properties of different Arctic ice types  
382 during the growth phase of MOSAiC: implications for future studies on gas pathways. *Frontiers in Earth*  
383 *Science*, **10**, 1-19.  
384 Battle, M., Bender, M. & Hendricks, M.B. (2003) Measurements and models of the atmospheric Ar/N<sub>2</sub> ratio.

- 385 *Geophysical Research Letters*, **30**, 1786.
- 386 Brown, K.A., Miller, L.A., Mundy, C.J. et al (2015) Inorganic carbon system dynamics in landfast Arctic sea ice  
387 during the early-melt period. *Journal of Geophysical Research: Oceans*, **120**, 3542-3566.
- 388 Buermann, W., Lintner, B.R., Koven, C.D. et al (2007) The changing carbon cycle at Mauna Loa Observatory.  
389 *Proceedings of the National Academy of Sciences*, **104**, 4249-4254.
- 390 Bushinsky, S.M., Gray, A.R., Johnson, K.S. et al (2017) Oxygen in the Southern Ocean from Argo floats:  
391 Determination of processes driving air-sea fluxes. *Journal of Geophysical Research: Oceans*, **122**, 8661–  
392 8682.
- 393 Bushinsky, S.M., Landschützer, P., Rödenbeck, C. et al (2019) Reassessing Southern Ocean air-sea CO<sub>2</sub> flux  
394 estimates with the addition of biogeochemical float observations. *Global Biogeochemical Cycles*, **33**, 1370-  
395 1388.
- 396 Cassar, N., McKinley, G.A., Bender, M.L. et al (2008) An improved comparison of atmospheric Ar/N<sub>2</sub> time series  
397 and paired ocean-atmosphere model predictions. *Journal of Geophysical Research*, **113**, D21122,
- 398 Ciais, P., Sabine, C., Bala, G. et al (2013) In: *Climate change 2013: the physical science basis. Contribution of*  
399 *Working Group I to the Fifth Assessment Report of the Intergovernmental Panel on Climate Change* (ed. by  
400 T. Stocker et al), pp. 465-570. Cambridge University Press, Cambridge, United Kingdom.
- 401 Dieckmann, G. S., Nehrke, G., Uhlig, C. et al (2010) Ikaite (CaCO<sub>3</sub>·6H<sub>2</sub>O) discovered in Arctic sea ice. *The*  
402 *Cryosphere*, **4**, 227–230
- 403 Fetterer, F., Knowles, K., Meier, W.N. et al (2017) Updated daily. Sea Ice Index, Version 3. monthly North and  
404 South. Boulder, Colorado USA. NSIDC: National Snow and Ice Data Center.  
405 <https://doi.org/10.7265/N5K072F8>. Accessed 26 February.
- 406 Geilfus, N.X., Carnat, G., Dieckmann, G.S. et al (2013) First estimates of the contribution of CaCO<sub>3</sub> precipitation to  
407 the release of CO<sub>2</sub> to the atmosphere during young sea ice growth. *Journal of Geophysical Research:*  
408 *Oceans*, **118**, 244-255.
- 409 Hamblar, C. (2017) Beyond physics: the advanced biology of climate change. *Climate Etc.*  
410 <https://judithcurry.com/2017/01/15/beyond-physics-advanced-biology-and-climate-change/>
- 411 Hamblar, C. and Henderson, P.A. (2020a) Sea ice and carbon dioxide. Working Paper. Version 2. Full text  
412 accessible on Oxford Research Archive (ORA) <[https://ora.ox.ac.uk/objects/uuid:640a0c7e-6b55-4aff-a9cc-](https://ora.ox.ac.uk/objects/uuid:640a0c7e-6b55-4aff-a9cc-f47f6b490254)  
413 [f47f6b490254](https://ora.ox.ac.uk/objects/uuid:640a0c7e-6b55-4aff-a9cc-f47f6b490254)>.
- 414 Hamblar, C. and Henderson, P.A. (2020b) Sea ice and methane. Working Paper. Full text accessible on Oxford  
415 Research Archive (ORA) <<https://ora.ox.ac.uk/objects/uuid:52b0e80f-7358-4b88-8941-55068738638e>>.
- 416 Hamblar, C. and Henderson, P.A. (2022) Temperature, carbon dioxide and methane may be linked through sea ice  
417 dynamics. *International Journal of Atmospheric and Oceanic Sciences*, **6**, 13-34.
- 418 Hamblar, C. (2022) Sea ice and oxygen. Preprint. Version 2. *Research Square*. [https://doi.org/10.21203/rs.3.rs-](https://doi.org/10.21203/rs.3.rs-2045347/v2)  
419 [2045347/v2](https://doi.org/10.21203/rs.3.rs-2045347/v2).
- 420 Hamme, R.C., and Emerson, S.R. (2002) Mechanisms controlling the global oceanic distribution of the inert gases  
421 argon, nitrogen, and neon. *Geophysical Research. Letters*, **29** (23) 2120.
- 422 Hamme, R. C., and S. R. Emerson (2004), The solubility of neon, nitrogen and argon in distilled water and seawater.  
423 *Deep-Sea Research I – Oceanographic Research Papers*, **51**, 1517–1528.
- 424 Ito, T. & Deutsch, C. (2006) Understanding the saturation state of argon in the thermocline: The role of air-sea gas  
425 exchange and diapycnal mixing. *Global Biogeochemical Cycles*, **20**, GB3019.
- 426 Ito, T., Hamme, R.C. & Emerson, S. (2011) Temporal and spatial variability of noble gas tracers in the North Pacific.  
427 *Journal of Geophysical Research: Oceans*, **116**, C08039.
- 428 Kawasaki, T. & Hasumi, H. (2016) The inflow of Atlantic water at the Fram Strait and its interannual variability.  
429 *Journal of Geophysical Research: Oceans*, **121**, 502-519.
- 430 Keeling, C.D. (1960) The concentration and isotopic abundances of carbon dioxide in the atmosphere. *Tellus*, **12**,  
431 200-203.
- 432 Keeling, C.D., Piper, S., Bacastow, R. et al (2001) Exchanges of atmospheric CO<sub>2</sub> and <sup>13</sup>CO<sub>2</sub> with the terrestrial  
433 biosphere and oceans from 1978 to 2000. In: *Exchanges of atmospheric CO<sub>2</sub> and <sup>13</sup>CO<sub>2</sub> with the terrestrial*  
434 *biosphere and oceans from 1978 to 2000. I. Global aspects, SIO Reference Series, No. 01-06*, pp. 1-88.  
435 Scripps Institution of Oceanography, San Diego.
- 436 Keeling, R.F. & Graven, H.D. (2021) Insights from time series of atmospheric carbon dioxide and related tracers.  
437 *Annual Review of Environment and Resources*, **46**, 85-110.
- 438 Keeling, R.F. & Manning, A.C. (2014) Studies of recent changes in atmospheric O<sub>2</sub> content. *Treatise on*

- 439 *Geochemistry, Volume 5* (ed. by R.F. Keeling & L. Russell), pp. 385-404. Elsevier, Amsterdam.
- 440 Lan, X., Dlugokencky, E.J., Mund, J.W., Crotwell A.M, Crotwell M.J., Moglia, E., Madronich M., Neff, D. &  
441 Thoning, K.W. (2022) Atmospheric Carbon Dioxide Dry Air Mole Fractions from the NOAA GML Carbon  
442 Cycle Cooperative Global Air Sampling Network, 1968-2021, Version: 2022-07-28,  
443 <https://doi.org/10.15138/wkgj-f215>.
- 444 Manning, A.C, Keeling, R.F., Katz, L.E. et al (2003) Interpreting the seasonal cycles of atmospheric oxygen and  
445 carbon dioxide concentrations at American Samoa Observatory. *Geophysical Research Letters*, **30**, 1333.
- 446 Moreau S., Vancoppenolle M., Zhou, J. et al (2014) Modelling argon dynamics in first-year sea ice. *Ocean*  
447 *Modelling*, **73**, 1-18.
- 448 Moreau, S., Vancoppenolle, M., Bopp, L. et al (2016) Assessment of the sea-ice carbon pump: Insights from a three-  
449 dimensional ocean-sea-ice biogeochemical model (NEMO-LIM-PISCES). *Elementa: Science of the*  
450 *Anthropocene*, **4**, 000122.
- 451 MOSAiC (2019) The key to the Arctic puzzle. from <https://www.mosaic-expedition.org/science/arctic-climate/>.  
452 Accessed 29 October 2019.
- 453 Nelson, M.D. & Nelson, D.B. (2016) Oceans, ice & snow and CO<sub>2</sub> rise, swing and seasonal fluctuation. *International*  
454 *Journal of Geosciences*, **7**, 1232-1282.
- 455 Nomura, D., Eicken, H., Gradinger, R. et al (2010) Rapid physically driven inversion of the air-sea ice CO<sub>2</sub> flux in  
456 the seasonal landfast ice off Barrow, Alaska after onset of surface melt. *Continental Shelf Research*, **30**,  
457 1998-2004.
- 458 Rysgaard, S., N. Glud, R.N., Sejr, M.K. et al (2007) Inorganic carbon transport during sea ice growth and decay: A  
459 carbon pump in polar seas. *Journal of Geophysical Research*, **112**, C03016.
- 460 Salby, M. (2012) *Physics of the atmosphere and climate*. 2nd edn. Cambridge University Press, Cambridge, United  
461 Kingdom.
- 462 Scripps O<sub>2</sub> Program (2022) <https://scripps2.ucsd.edu/index.html>. Accessed 29 August 2022.
- 463 Semiletov, I.P., Pipko, I.I., Repina, I. et al (2007) Carbonate chemistry dynamics and carbon dioxide fluxes across  
464 the atmosphere-ice-water interfaces in the Arctic Ocean: Pacific sector of the Arctic. *Journal of Marine*  
465 *Systems*, **66**, 204-226.
- 466 Shuchman, R.A., Josberger, E.G., Russel, C.A. et al (1998) Greenland Sea Odden sea ice feature: Intra-annual and  
467 interannual variability. *Journal of Geophysical Research*, **103**, 12,709-12,724.
- 468 Sjøgaard, D.H., Thomas, D.N., Rysgaard, S. et al (2013) The relative contributions of biological and abiotic processes  
469 to carbon dynamics in subarctic sea ice. *Polar Biology*, **36**, 1761-1777.
- 470 Stanley, R.H.R., Jenkins, W.J., Lott III D.WE. et al (2009) Noble gas constraints on air-sea gas exchange and bubble  
471 fluxes. *Journal of Geophysical Research*, **114**, C11020.
- 472 Tison, J.-L., Delille, B. & Papadimitriou, S. (2016) Gases in sea ice. In: *Sea ice*, 3rd edn. (ed. by D.N. Thomas), pp.  
473 433-471. Wiley, New Jersey.
- 474 Trainer, M.G., Wong, M.H. McConnochie, T.H. et al. (2019) Seasonal variations in atmospheric composition as  
475 measured in Gale Crater, Mars. *Journal of Geophysical Research: Planets*, **124**, 3000-3024.
- 476 Vancoppenolle, M., Goosse, H., de Montety, A. et al (2010) Modeling brine and nutrient dynamics in Antarctic sea  
477 ice. The case of dissolved silica. *Journal of Geophysical. Research: Oceans*, **115**, C02005.
- 478 Vancoppenolle, M., Meiners, K.M., Michel, C. et al (2013) Role of sea ice in global biogeochemical cycles:  
479 emerging views and challenges. *Quaternary Science Reviews*, **79**, 207-230.
- 480 Vancoppenolle, M. & Tedesco, L. (2016) Numerical models of sea ice biogeochemistry. In: *Sea ice*, 3rd edn. (ed. by  
481 D.N. Thomas), pp. 492-515. Wiley, New Jersey.
- 482 Zhou, J., Delille, B., Eicken, H. et al (2013) Physical and biogeochemical properties in landfast sea ice (Barrow,  
483 Alaska): insights on brine and gas dynamics across seasons. *Journal of Geophysical Research: Oceans*, **118**,  
484 3172-3189.